2011

CD103+ pulmonary dendritic cells preferentially acquire and present apoptotic cell-associated antigen

A Nicole Desch

Gwendalyn J. Randolph

Kenneth Murphy

Emmanuel L. Gautier

Ross M. Kedl

See next page for additional authors

Authors

A Nicole Desch, Gwendalyn J. Randolph, Kenneth Murphy, Emmanuel L. Gautier, Ross M. Kedl, Mireille H. Lahoud, Irina Caminschi, Ken Shortman, Peter M. Henson, and Claudia V. Jakubzick

CD103+ pulmonary dendritic cells preferentially acquire and present apoptotic cell–associated antigen

A. Nicole Desch,[3] Gwendalyn J. Randolph,[4,5] Kenneth Murphy,[6] Emmanuel L. Gautier,[4,5] Ross M. Kedl,[3] Mireille H. Lahoud,[7,8] Irina Caminschi,[7] Ken Shortman,[7,8] Peter M. Henson,[1,2,3] and Claudia V. Jakubzick[1,3]

[1]Department of Pediatrics, [2]Department of Medicine, and [3]Integrated Department of Immunology, National Jewish Health, University of Colorado Denver, Denver, CO 80206
[4]Department of Development Regenerative Biology and [5]Immunology Institute, Mount Sinai School of Medicine, New York, NY 10029
[6]Department of Pathology and Immunology, Washington University in St. Louis School of Medicine, St. Louis, MO 63130
[7]The Walter and Eliza Hall Institute of Medical Research, Parkville, Victoria 3052, Australia
[8]Department of Medical Biology, The University of Melbourne, Melbourne, Victoria 3010, Australia

Cells undergoing programmed cell death (apoptosis) are removed in situ by macrophages and dendritic cells (DCs) through a specialized form of phagocytosis (efferocytosis). In the lung, there are two primary DC subsets with the potential to migrate to the local lymph nodes (LNs) and initiate adaptive immune responses. In this study, we show that only CD103+ DCs were able to acquire and transport apoptotic cells to the draining LNs and cross present apoptotic cell–associated antigen to CD8 T cells. In contrast, both the CD11bhi and the CD103+ DCs were able to ingest and traffic latex beads or soluble antigen. CD103+ DCs selectively exhibited high expression of TLR3, and ligation of this receptor led to enhanced in vivo cytotoxic T cell responses to apoptotic cell–associated antigen. The selective role for CD103+ DCs was confirmed in Batf3−/− mice, which lack this DC subtype. Our findings suggest that CD103+ DCs are the DC subset in the lung that captures and presents apoptotic cell–associated antigen under homeostatic and inflammatory conditions and raise the possibility for more focused immunological targeting to CD8 T cell responses.

CORRESPONDENCE
Claudia Jakubzick:
jakubzickc@njhealth.org

Abbreviations used: i.n., intranasal(ly); LLN, lung-draining LN; mRNA, messenger RNA; PBSE, Pacific blue succinimidyl ester; PI, propidium iodide; sOVA, soluble OVA.

Pulmonary DCs are the critical APCs that recognize and capture all types of antigens in the lung. They then ferry and present these antigens in the lung-draining LN (LLN). These antigens include viruses, bacteria, fungi, and even in the case of autoimmunity, self-antigens. Despite their essential roles, very little is known about the basic mechanisms or selectivity by which pulmonary DCs acquire pathogens or host cells and how they subsequently regulate the immune response.

Three DC types have been described in the naive lung: plasmacytoid DCs and two migratory DCs, CD103+ and CD11bhi DCs (Vermaelen and Pauwels, 2004; Sung et al., 2006; Jakubzick et al., 2008a). The functional roles of pulmonary DC subsets are beginning to unfold (Plantinga et al., 2010). An in vitro study extracting LLN migratory DCs containing soluble OVA (sOVA) suggested that pulmonary CD103+ DCs could cross-present antigens on MHC class I, whereas CD11bhi DCs were responsible for antigen presentation on MHC class II (Belz et al., 2007; del Rio et al., 2007). In vivo studies, using deletion approaches and transcription factor knockout mice for the depletion of DC subsets, revealed that pulmonary CD103+ DCs are required for a CTL response to viruses (GeurtsvanKessel et al., 2008; Kim and Braciale, 2009; Edelson et al., 2010). Yet it remains unclear how the DCs acquired the virus for presentation. DCs may take up virus directly or by ingestion of an infected cell such as a dying epithelial cell. Recognition and removal of cells undergoing apoptosis and other forms of

The Rockefeller University Press $30.00
J. Exp. Med. Vol. 208 No. 9 1789-1797
www.jem.org/cgi/doi/10.1084/jem.20110538

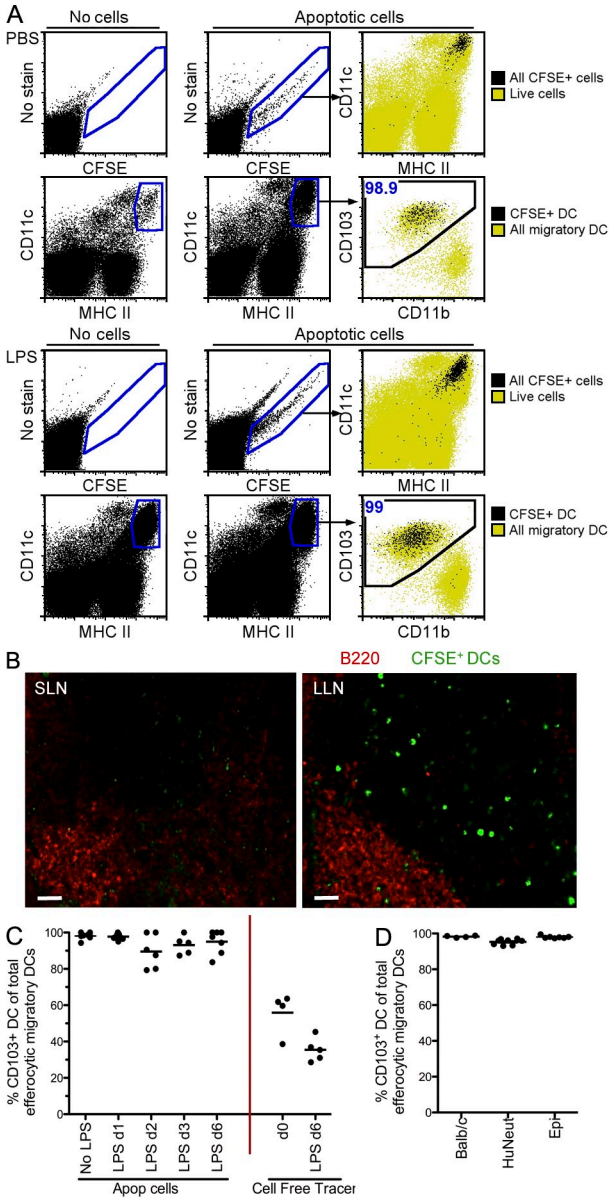

Figure 1. Apoptotic cell trafficking to the LLN by lung CD103⁺ DCs. (A) C57BL/6 mice were inoculated i.n. with CFSE-labeled apoptotic thymocytes in the absence (top) or presence (bottom) of 2 µg LPS. Control mice received no cells. LLN cells were isolated 24 h later and analyzed by flow cytometry. Efferocytic cells were identified as CFSE⁺, and migratory DCs were identified as CD11c⁺MHCII^{hi}. Overlays show CFSE⁺ cells (black) and total live cells or total migratory DCs (yellow) as indicated. Numbers indicate frequency of CFSE⁺ DCs that express CD103. Representative data of four independent experiments with three mice/group are shown. (B) Skin-draining LNs (SLNs) and LLNs were sectioned 24 h after delivery of CFSE-labeled apoptotic thymocytes. Tissue sections were stained with anti-B220 (red) and CFSE (green). Bars, 40 µm. (C) 24 h after i.n. delivery of CFSE-labeled apoptotic thymocytes, the frequency of CD103⁺ DCs among total CFSE⁺ cells was calculated in the LLN during the indicated times throughout an acute inflammatory response. As a control, PKH 26 cell-free tracer was used to track migratory DCs to the LLN. Data represent the results of three independent experiments. (D) C57BL/6 mice were inoculated i.n. with CFSE-labeled apoptotic BALB/c thymocytes, human neutrophils, or murine lung epithelial cell line (MLE 12). Uptake by migratory DCs was accessed 24 h later. (C and D) Each dot represents an individual mouse. Bars represent the mean of the individual mice per group.

programmed cell death occur by specific recognition of ligands and uptake processes termed efferocytosis (deCathelineau and Henson, 2003), a property which is shared by macrophages and some subsets of DCs. Thus, within the splenic DC populations, CD8⁺ DCs selectively acquire apoptotic cells. This selectivity was also observed in nonlymphoid DC subsets in mouse liver and rat intestine (Iyoda et al., 2002; Qiu et al., 2009); however, the expression of CD103 was not investigated. Moreover, there is indirect evidence that CD103⁺ DCs in the skin capture self-apoptotic cells during homeostasis (Bedoui et al., 2009). CD103⁺ DCs, including pulmonary CD103⁺ DCs, share many similar properties with the lymphoid CD8⁺ DCs of the spleen, including developmental regulation by Flt3 and transcription factors Irf8 and Batf3 (Edelson et al., 2010), and the capacity to cross-present antigen. However, besides their differences in location, there is one property they do not share, which is the capacity to migrate down afferent lymphatics (Smith and Fazekas de St Groth, 1999). The finding that not all DCs migrate to the draining LN when injected into nonlymphoid sites such as the skin further supports the need to understand the functional roles of tissue-resident DCs.

Accordingly, to delineate functional roles of the different pulmonary DCs, we set out to identify which migratory DC population was capable of acquiring apoptotic cells in the tissue for presentation of contained antigen in the LLN. We hypothesized and now show that pulmonary CD103⁺ DCs selectively express TLR3 and exhibit preferential uptake and trafficking of apoptotic cells compared with the CD11b^{hi} DCs. Furthermore, only the CD103⁺ migratory DCs were capable of cross-presenting airway apoptotic cell–associated antigen in the LLN.

RESULTS AND DISCUSSION

CD103⁺ DCs but not CD11b^{hi} DCs selectively traffic apoptotic cells to the draining LN

Intranasal (i.n.) delivery of CFSE-labeled apoptotic thymocytes showed that of the migratory DCs in the draining LNs, only CD103⁺ DCs captured apoptotic cells (Fig. 1 A). This was true whether or not LPS was included in the instillate to enhance DC migration (Jakubzick et al., 2008a). Furthermore, essentially all the CFSE⁺ cells were located within the CD103⁺CD11c⁺MHCII^{hi} migratory DC population assessed by FACS, and nearly all efferocytic cells were localized to the T cell zone of the LLN by immunohistochemistry (Fig. 1, A and B). This selectivity was striking because our previous study showed that bead particles, soluble protein, and free CFSE delivered i.n. are trafficked to the LLN by both pulmonary CD103⁺ and CD11b^{hi} DCs (Jakubzick et al., 2008a). Importantly, apoptotic cells in the lung, for example during resolution of inflammation, can be taken up by alveolar macrophages

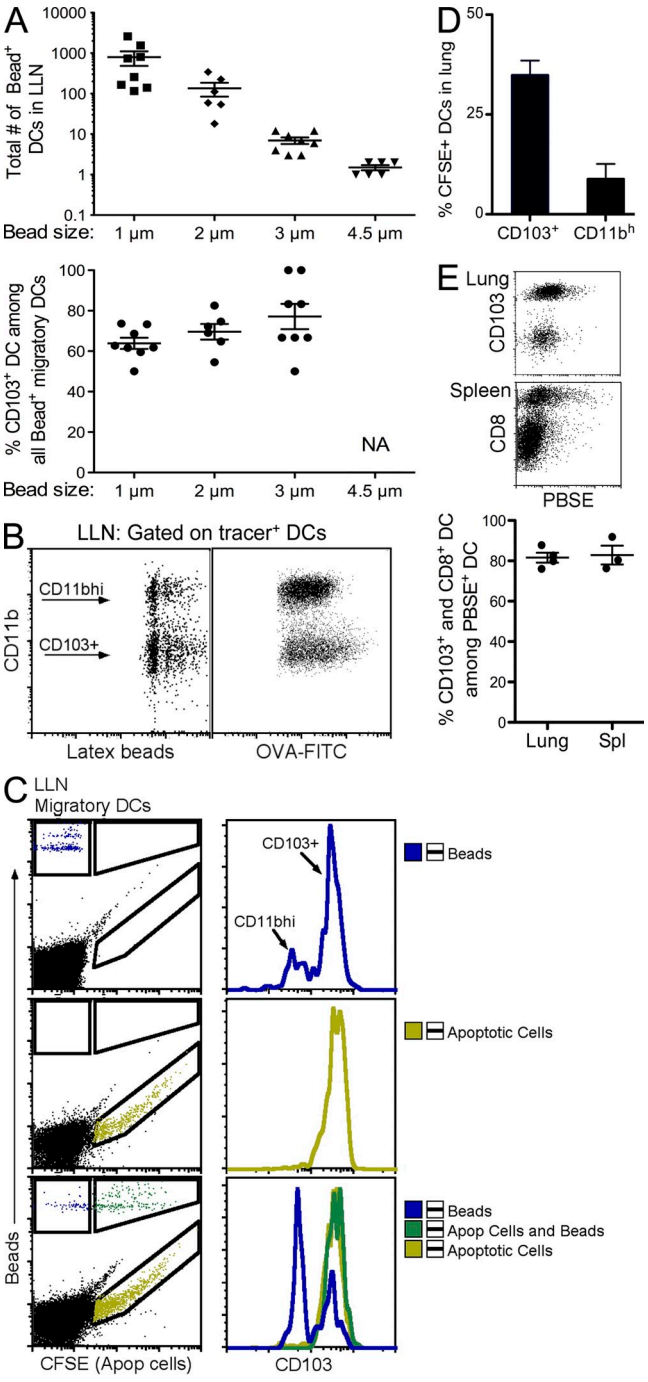

Figure 2. CD103⁺ DCs preferentially take up apoptotic cells, whereas both CD103⁺ and CD11b^{hi} cells take up particulate beads. (A) C57BL/6 mice were inoculated i.n. with 30 × 10⁶ latex beads of the indicated size, and the total number of bead⁺ cells (top) or frequency of CD103⁺ DC among all bead⁺ cells (bottom) was determined 24 h later. NA indicates not quantitated because of the paucity of migrated beads. Data shown are representative of three independent experiments. Mean ± SEM is shown. (B) C57BL/6 mice were inoculated i.n. with 30 × 10⁶ latex beads (1 µm) or OVA-FITC, and 24 h later, LLN bead⁺ or OVA-FITC⁺ migratory DCs were analyzed by flow cytometry. (C) LLNs were harvested from mice inoculated with beads alone (top), CFSE-labeled apoptotic cells (middle), and beads with CFSE-labeled apoptotic cells (bottom). LLNs were gated on bead⁺ cells (blue), CSFE⁺ cells (yellow), or CSFE⁺bead⁺ cells (green). Histograms show CD103 expression on gated cells (CD103^{lo} = CD11b^{hi} DCs; CD103^{hi} = CD103⁺ DCs). Data are representative of two independent experiments with three mice/group. (D) Lung tissue was harvested 2 h after i.n. inoculation with CFSE-labeled apoptotic cells, and the frequency of the indicated DC subsets was determined by flow cytometry. Data are representative of three independent experiments. Error bars indicate SEM. (E) CD103⁺ or CD8⁺ DCs were isolated from lungs (top) and spleen (middle) and cultured with PBSE-labeled apoptotic cells for 4 h. The frequency of apoptotic cell uptake for each population among total PBSE⁺ DCs was calculated (bottom). Each dot represents the mean of triplicates from three independent experiments. Error bars indicate SEM.

as well as by DCs, a competitive effect which required administration of large enough numbers of apoptotic cells to overcome this potential competition.

It was possible that CD11b^{hi} DCs might gain the property of efferocytosis during an acute inflammatory response, either from the change in milieu and/or because a quantitative advantage exists for CD11b^{hi} DCs when they preferentially accumulate in the lung during inflammation (Kirby et al., 2006; GeurtsvanKessel et al., 2008, 2009; Kim and Braciale, 2009; Lukens et al., 2009; Ballesteros-Tato et al., 2010). Accordingly, inflammation was induced by i.n. delivery of 2 µg LPS 6, 3, 2, or 1 d before delivery of CFSE-labeled apoptotic cells. 24 h after apoptotic cell delivery, DCs were analyzed for uptake and trafficking of CFSE⁺ apoptotic cells to the LLN. However, regardless of the time apoptotic cells were introduced within an acute inflammatory environment, CD103⁺ DCs were consistently found to preferentially transport apoptotic cells to the LLN (Fig. 1 C). Therefore, even in the context of acute inflammation where epithelial permeability is enhanced, CD11b^{hi} DCs do not contribute substantially to the trafficking of apoptotic cells to the LLN.

To ascertain whether the acquisition and trafficking of apoptotic cells by CD103⁺ DCs was conserved using different apoptotic cell sources, C57BL/6 mice were given CFSE-labeled apoptotic BALB/c thymocytes, human neutrophils, or murine lung epithelial cells and analyzed for CFSE⁺ migratory DCs in the LLN 24 h later. Even when mouse strains and species were incongruent, pulmonary CD103⁺ DCs still maintained their selectivity for the transport of apoptotic cells to the LLN (Fig. 1 D and Fig. S1). Overall, these data demonstrate that CD103⁺ DCs are efferocytic.

CD103⁺ DCs preferentially localize along the airways and line the vasculature (Sung et al., 2006). Because there might be a locational advantage that allows CD103⁺ DCs to acquire apoptotic cells, co-delivery of particulate beads and apoptotic cells was examined. Initial experiments assessed the uptake and trafficking of 1-, 2-, 3-, and 4.5-µm diameter latex beads administered along with LPS to enhance DC migration and allow detection of larger size beads in the draining LN (Jakubzick et al., 2008a). As expected, both migratory pulmonary DC subsets transported the beads to the draining LNs; however, the frequency of bead-positive CD103⁺ DCs slightly increased as bead size increased (Fig. 2 A). Unlike apoptotic

cells, beads are not malleable, therefore it may not be surprising that beads as large as 7-µm cells were not transported to the LLNs. Detectable DC transport of beads was limited to 3-µm beads or smaller, as very few bead-carrying cells were found in LNs when ≥4.5-µm particles were instilled. Most notably, with 0.5- and 1-µm beads, CD103$^+$ DCs not only trafficked beads at a greater frequency, but also quantitatively carried more beads per cell than CD11b^{hi} DCs (Fig. 2 B and not depicted for 0.5 µm). The same quantitative observation was made for sOVA protein. That is, even though we have previously shown that CD11b^{hi} DCs traffic sOVA at a higher frequency than CD103$^+$ DCs (Jakubzick et al., 2008a), some CD103$^+$ DCs have quantitatively more OVA per cell than CD11b^{hi} DCs (Fig. 2 B). Thus, in general, CD103$^+$ DCs appear to be more endocytic than CD11b^{hi} DCs. Because 3-µm beads were the limiting bead size for DC trafficking, 2-µm beads were chosen for co-delivery experiments with apoptotic cells.

Co-delivery of apoptotic cells i.n. along with 2-µm latex beads revealed that CD103$^+$ DCs either trafficked apoptotic cells alone or apoptotic cells with beads to the LLN. In contrast, CD11b^{hi} DCs carried beads but not apoptotic cells to the LLN (Fig. 2 C). Because these data show that nonspecific airway particulates can be engulfed and transported by CD11b^{hi} DCs as well as CD103$^+$ DCs to the LLN, the specificity of the CD103$^+$ DCs in efferocytosis was not caused by failure of CD11b^{hi} DCs to access phagocytic cargo.

Selective uptake of apoptotic cells by CD103$^+$ DCs in the lung tissue

To determine whether the selectivity for apoptotic cell trafficking to the LLN occurred at the level of recognition and uptake by DCs in the lung, lungs were harvested, and DCs were sorted 2 h after i.n. delivery of the tagged apoptotic cells. By immunofluorescence analysis, 30% of total lung CD103$^+$ DCs had associated apoptotic cell bodies compared with 7% of CD11b^{hi} DCs (Fig. 2 D). The observation that after isolation from the lung, a few CD11b^{hi} CD11c^{hi}MHCII^{hi} cells contained apoptotic cells after cell sorting, whereas in the draining LN only CD103$^+$ DCs contained apoptotic cells, suggests a possible explanation that CD11b^{hi}CD11c^{hi}MHCII^{hi} DCs represent a heterogeneous population containing other monocytic-like cells, not yet identified, that can bind and/or ingest apoptotic cell bodies, which are unable to migrate to the LLN.

Moreover, in vitro uptake of apoptotic cells by pulmonary DCs was assessed. In culture, pulmonary CD103$^+$ DCs preferentially acquired apoptotic cells over CD11b^{hi} DCs, albeit with less efficiency than splenic CD8$^+$ DCs (Fig. 2 E). Putting the data together, we demonstrated that at the level of the lung parenchyma, CD103$^+$ DCs appear selectively specialized to engulf apoptotic cells and subsequently transport these to the LLN.

CD103$^+$ DCs cross-present apoptotic cell–associated antigen

Pulmonary CD103$^+$ DCs have been directly shown in vitro to be specialized in cross-presentation (Belz et al., 2007; del Rio et al., 2007). Because we have demonstrated in vivo a selective uptake of apoptotic cells by CD103$^+$ DCs, the selective ability of these cells to cross present antigen in vivo was next examined using apoptotic thymocytes

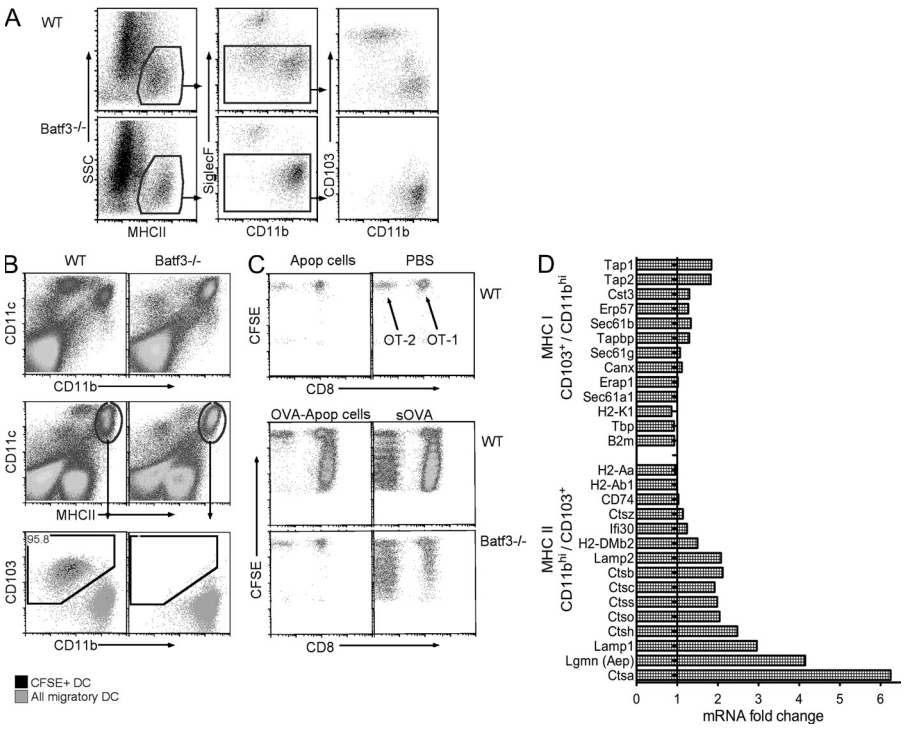

Figure 3. Efferocytic pulmonary CD103$^+$ DCs are required for apoptotic cell acquisition, migration to the LLN, and cross-presentation. (A) Lung DC subsets from WT and Batf3$^{-/-}$ mice were gated on CD11c$^+$ and analyzed by flow cytometry for expression of MHCII, CD11b, and CD103. Cell were gated on MHCII$^+$ (left) and SiglecF$^-$ (middle) and plotted for CD11b and CD103 expression (right). (B) LLNs were isolated from WT and Batf3$^{-/-}$ mice 24 h after inoculation with CFSE-labeled apoptotic cells. Cells were gated on live cells and analyzed for CD11c versus CD11b (top) or MHCII (bottom). Overlay plots show CFSE$^+$ DCs (black) and all migratory DCs (gray). Data are representative of two independent experiments with three mice/group. (C) WT and Batf3$^{-/-}$ mice were inoculated with a 1:1 mixture of CFSE-labeled OT-1 and OT-2 cells (2×10^6 total cells) 1 d before i.n. delivery of apoptotic WT cells, PBS, apoptotic OVA-expressing cells, or 1 µg sOVA. T cell proliferation was assessed 3 d later. Data are representative of three independent experiments with two to three mice/group. (D) DC subsets were isolated from PBS-perfused lung tissue, and mRNA was isolated for microarray analysis. Plots show fold change of the indicated genes in pulmonary CD103$^+$ DCs versus CD11b^{hi} DCs (top) or pulmonary CD11b^{hi} DCs versus CD103$^+$ DCs (bottom).

isolated from OVA-expressing mice (OVA apoptotic thymocytes). To examine the CD103$^+$ DC specificity for cross-presentation of cell-associated antigen, Batf3$^{-/-}$ mice were used. Batf3$^{-/-}$ mice lack lymphoid CD8$^+$ DCs and non-lymphoid CD103$^+$ DC in multiple tissues including the lung and LLN (Fig. 3, A and B; Hildner et al., 2008; Edelson et al., 2010). As shown in Fig. 3 B, the lack of CD103$^+$ DCs and trafficked CFSE-labeled apoptotic cells in LLN in the Batf3$^{-/-}$ mice confirmed the requirement for this DC type.

Next, apoptotic cell–associated antigen presentation was assessed by CD103$^+$ DCs. Mice were given i.v. a 1:1 ratio of CFSE-labeled OVA-specific OT-1 (CD8) and OT-2 (CD4) transgenic T cells 1 d before i.n. delivery of OVA-apoptotic thymocytes or sOVA. 3 d later, proliferation of OVA-specific T cells was measured. Strikingly, antigen from OVA apoptotic thymocytes was presented exclusively to CD8 T cells (Fig. 3 C). In contrast, instillation of sOVA induced both OT-1 and OT-2 proliferation, i.e., both pulmonary DCs acquired and presented the antigen (Figs. 2 B and 3 C; Jakubzick et al., 2008a). Thus, only the pulmonary CD103$^+$ DC acquired and trafficked apoptotic cell–associated antigen and led to its cross-presentation to antigen-specific CD8 T cells. Unlike WT mice, presentation of apoptotic cell–associated antigen to either OT-1 or OT-2 T cells did not occur in Batf3$^{-/-}$ mice (Fig. 3 C), further confirming the role for CD103$^+$ DCs. However, this experiment does not exclude a possible role for lymphoid CD8$^+$ DCs (also absent in the Batf3$^{-/-}$ mice) for antigen presentation after CD103$^+$ DCs transport antigen and arrive in the draining LN (Belz et al., 2004). Delivery of sOVA led to a skewed proliferative response of OT-2 T cells in the Batf3$^{-/-}$ mice compared with WT mice, whereas in the WT mice the OT-1 T cell response was stronger, which is most likely attributable to the enhanced antigen trafficking and cross-presentation by the CD103$^+$ DCs (Fig. 3 C).

Because pulmonary CD103$^+$ DCs, along with splenic CD8$^+$ DCs, favor apoptotic cell uptake and cross-presentation, we examined levels of gene expression in the MHC class I and MHC class II pathway molecules in the former, as previously reported for splenic DCs (Dudziak et al., 2007). Indeed, pulmonary CD103$^+$ DCs demonstrated enhanced gene expression for MHC class I pathway molecules, whereas CD11b^{hi} DCs displayed enhanced expression in several of the MHC class II pathway molecules (Fig. 3 D). The observation supports the suggested intrinsic capacity of CD103$^+$ DCs to cross-present antigen, whereas CD11b^{hi} DCs appear more effective at presentation via MHC class II. However, these findings do not negate the ability for both pulmonary DCs to use all of the antigen-presenting pathways.

Cell-associated antigen presentation by CD103$^+$ DCs along with TLR3 agonist enhances IFN-γ production and cytotoxicity from the proliferating OT-1 T cells

Unlike CD11b^{hi} DCs, CD103$^+$ DCs demonstrated selective expression of TLR3, along with CCR9, CXCR3, XCR1, and Cadm1 (Fig. 4 A and Table S1). In contrast, CD11b^{hi} DCs expressed Clec4a1, TLR2, and TLR7 (Fig. 4 A and Table S1). The data suggest a differential ability of the DC types to recognize and respond to pathogens.

TLR3 recognizes viral double-stranded RNA and is specifically expressed by CD103$^+$ DCs. Therefore, we examined the ability of Poly I:C, a TLR3 agonist, to enhance IFN-γ production in proliferating OT-1 T cells after apoptotic cell–associated antigen and soluble antigen presentation. Mice treated with Poly I:C and OVA apoptotic cells did not promote

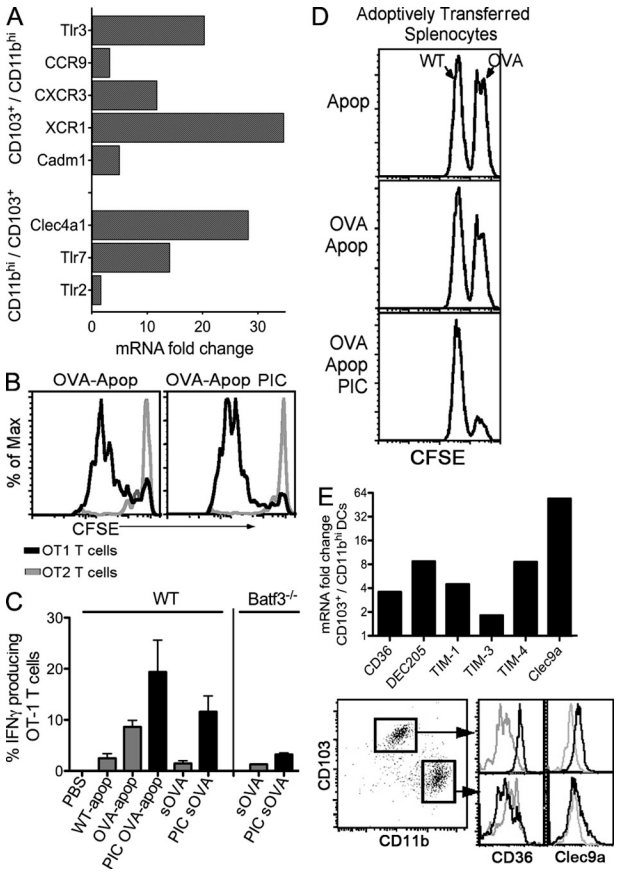

Figure 4. CD103$^+$ DCs selectively express TLR3, which promotes IFN-γ production and CTL responses. (A) Expression of the indicated genes in pulmonary CD103$^+$ DCs versus CD11b^{hi} DCs (top) and pulmonary CD11b^{hi} DCs versus CD103$^+$ DCs (bottom). (B and C) WT (B) and Batf3$^{-/-}$ (C) mice were inoculated with a 1:1 mixture of CFSE-labeled OT-1 and OT-2 cells (2×10^6 total cells) 1 d before i.n. delivery of apoptotic OVA ± 10 µg Poly I:C (B) and apoptotic WT or OVA-expressing cells or sOVA ± 10 µg Poly I:C (C). 3 d later, the cells were assessed for proliferation (B) or IFN-γ production (C). Data are representative of two independent experiments. Error bars indicate SEM. (D) OT-1 cells (1×10^6 total cells) were transferred into WT mice 1 d before inoculation with WT or OVA-expressing apoptotic cells ± 10 µg Poly I:C. 5 d later, mice were injected with a 1:1 ratio of CFSE^{lo}-labeled WT and CFSE^{hi}-labeled OVA$^+$ splenocytes. The presence of CFSE^{lo} and CFSE^{hi} cells was assessed by flow cytometry 24 h later. Data are representative of two independent experiments with three mice/group. (E) Expression of the indicated genes in pulmonary CD103$^+$ DCs versus CD11b^{hi} DCs (top). Protein expression of CD36 and Clec9a (black line) on the indicated pulmonary DC subsets was analyzed by flow cytometry. Isotype control is indicated by the gray line. Gene expression analysis was performed on DC populations isolated independently on three separate days.

MHCII cell–associated antigen presentation (Fig. 4 B) but instead induced three times more IFN-γ–producing OT-1 T cells compared with mice treated with OVA apoptotic cells alone (Fig. 4 C). sOVA in the presence of Poly I:C showed six times more IFN-γ–producing OT-1 T cells compared with mice given sOVA alone (Fig. 4 C). In contrast, this enhancement was not observed in the Batf3$^{-/-}$ mice, i.e., lacking the TLR3-expressing CD103^{+} DCs (Fig. 4 C). Thus, these data suggest that Poly I:C–induced IFN-γ production by antigen-specific CD8 T cells required the presence and antigen presentation of CD103^{+} DCs.

This evidence of CD8 T cell activation suggests a comparable induction of cytotoxicity in the proliferating OT-1 T cells. To examine this, OT-1 T cells were adoptively transferred into mice 1 d before i.n. delivery of WT apoptotic thymocytes (as control) or OVA apoptotic thymocytes with PBS or with 10 µg Poly I:C. 5 d later, WT splenocytes and OVA-expressing splenocytes were labeled with a low and high concentration of CFSE, respectively, and then delivered i.v. at a 1:1 ratio as targets for the measurement of antigen-specific cytotoxicity. 24 h after splenic cell delivery, mice were assessed for their cytotoxic response to OVA-expressing splenocytes. Mice treated with WT apoptotic thymocytes displayed equal ratios of WT and OVA-expressing splenocytes (Fig. 4 D). Mice treated with OVA apoptotic thymocytes alone displayed slight cytotoxicity toward the OVA-expressing splenocytes. In contrast, there was almost complete ablation of OVA-expressing splenocytes in mice treated with OVA apoptotic thymocytes and Poly I:C (Fig. 4 D). These data demonstrated that the addition of Poly I:C with apoptotic cells enhanced the cytotoxicity of antigen-specific T cells.

Overall, pulmonary CD103^{+} DCs and splenic CD8^{+} DCs share multiple attributes including growth factors and transcription factors that regulate them, chemokine and pattern recognition receptor expression, and functional properties such as preferential uptake of apoptotic cells and cross-presentation. However, there is one major functional difference between the nonlymphoid and lymphoid DCs: CD103^{+} DCs migrate down afferent lymphatics, whereas CD8^{+} DCs do not (Fig. S2 A; Smith and Fazekas de St Groth, 1999). There is a study that has shown that peptide-pulsed CD8^{+} and CD8^{-} splenic DCs elicit opposing immune responses (Maldonado-López et al., 1999). Because we and others show that splenic CD8^{+} DCs do not migrate down afferent lymphatics, the immunological outcome observed by the delivery of peptide-pulsed splenic CD8^{+} DCs may have been caused by the acquisition of dying CD8^{+} DCs by endogenous skin efferocytic DCs that cross-present in the draining LN (Bedoui et al., 2009). In contrast, CD8^{-} DCs, either CX3CR1^{hi} or CX3CR1^{lo} (Fig. S2 B), do migrate to draining LNs to present the peptide-pulsed antigen, leading to the immunological outcome observed (Smith and Fazekas de St Groth, 1999). The inability of splenic CD8^{+} DCs to migrate should caution the use of its human DC orthologue; for instance, if human blood CD141^{+} DCs were antigen pulsed and adoptively transferred into the dermis of patients, their lymphatic migratory capacity would need to be investigated. Alternatively, when designing organ-specific vaccines, perhaps targeting tissue-resident DCs might prove to be more efficacious.

It was unexpected that CD11b^{hi} DCs under the conditions studied would neither acquire nor traffic apoptotic cells to the LLN because unlike splenic CD8^{-} DCs, CD11b^{hi} DCs arise from the monocytic linage that gives rise to macrophages (Landsman et al., 2007; Jakubzick et al., 2008b; Ginhoux et al., 2009). Therefore, there appears to be a dichotomy between the monocytic DC and macrophage, in which macrophages efferocytose with greater efficiency than pulmonary CD11b^{hi} DCs. Even though CD11b^{hi} DCs do not appear to contribute substantially to airway apoptotic cell clearance, this finding does not negate the possibility that CD11b^{hi} DCs could acquire apoptotic or necrotic cells, or cellular contents, during an infection where some studies have demonstrated that in the LLN CD11b^{hi} DCs in vitro can cross-present flu antigens (GeurtsvanKessel et al., 2009; Kim and Braciale, 2009; Ballesteros-Tato et al., 2010). Influenza is a lytic virus providing CD11b^{hi} DCs with free virions and necrotic cell debris. Alternatively, CD11b^{hi} DCs could be cross-dressed because a recent study demonstrated that splenic CD8^{-} DCs were more efficiently cross-dressed than CD8^{+} DCs (Wakim and Bevan, 2011).

In conclusion, we demonstrate a major functional difference between the two pulmonary DC subsets, a selective skewing of apoptotic cell uptake by CD103^{+} DCs, and subsequent cross-presentation of associated antigen. Lack of the CD103^{+} DCs in the Batf3$^{-/-}$ mice prevented cross-presentation. These experiments suggest that a major determinant in this selectivity resides in the initial recognition and uptake of the apoptotic cells by DC subsets within the lung parenchyma. There are a host of potential receptors for apoptotic cell ligands that have been identified on phagocytes, including DCs, and future studies will need to identify these on the different DC subsets. Examination of the microarray screen of CD103^{+} versus CD11b^{hi} DCs showed increased levels of messenger RNA (mRNA) for candidates such as CD36, DEC205, TIM-1, TIM-3, TIM-4, and Clec9a. CD36 and Clec9a were confirmed by cell surface protein levels (Fig. 4 E and Table S1), which may provide a starting point for such investigation.

Accordingly, pulmonary CD103^{+} DCs are an attractive DC subtype to exploit in strategies to potentiate peripheral tolerance, or antiviral and antitumor immunity, given their intrinsic ability to engulf apoptotic cells, migrate to LNs, cross-present cellular antigen, and, with Poly I:C, promote cytotoxicity.

MATERIALS AND METHODS

Mice. CD45.1 and CD45.2 C57BL/6, 129/BL6 F2 (control for Batf3$^{-/-}$ mice) OT-1, OT-2, CX3CR1$^{gfp/gfp}$, and C57BL/6-Tg(ACTB-OVA)916Jen/J mice were purchased from Jackson ImmunoResearch Laboratories, Inc. Batf3$^{-/-}$ mice were provided by K. Murphy. Mice were used for experiments at 7–8 wk of age, housed in a specific pathogen-free environment at National Jewish Health, and used in accordance with protocols approved by the Institutional Animal Care and Utilization Committee.

Flow cytometry. Single-cell suspensions were obtained from whole lung, spleen, and LLN. All LLN data were individually harvested, not pooled, and analyzed. Prior to lung extraction, mice were perfused with 10 ml PBS.

All tissues were minced and then digested with 2.5 mg/ml collagenase D (Roche) for 30 min at 37°C. 100 µl of 100 mM EDTA was added to stop the digestion, and then the tissue was collected using a glass Pasteur pipette and pressed through a 100-µm nylon strainer for single-cell suspension. Spleens were treated with 7.5 ml of ammonium chloride lysing reagent (BD), followed rapidly by the addition of 7.5 ml HBSS. Cells were resuspended in FACS blocking solution and stained for 30 min with conjugated antibodies obtained from eBioscience and BD. The following purified mAbs were used for staining: Pacific blue–conjugated mAbs to CD8 and I-A/I-E; PE-conjugated mAbs to I-A/I-E, Siglec F, CD11b, CD8, or CD103; PerCP-Cy5.5–conjugated mAbs to CD4 or CD11b; PE-Cy7–conjugated mAb to CD11c; and allophycocyanin-conjugated mAbs to CD103. CD36 was purchased from BioLegend, and biotin-conjugated mAb to Clec9a was provided by M.H. Lahoud, I. Caminschi, and K. Shortman (Caminschi et al., 2008). Appropriate isotype-matched control mAbs were also obtained from eBioscience, BD, and BioLegend. Flow cytometry was performed using the LSR II (BD), and data were analyzed with FlowJo (Tree Star).

Immunostaining. Frozen sections of the LLN and skin brachial-LN were fixed in 4% paraformaldehyde and stained with Cy5-B220 (eBioscience) or isotype-matched control antibody.

i.n. deliveries. Administration of i.n. deliveries was performed using an optimized delivery system previously described (Jakubzick et al., 2008a; Jakubzick and Randolph, 2010). In brief, mice were completely anesthetized with Avertin using 300 µl per mouse with *tert*-amyl alcohol content at 2.5% and 2,2,2 tribromoethanol (T1420; TCI America) at a concentration of 50 mg/kg. Cells or beads were diluted in PBS, and 50 µl of solution was delivered i.n. Final concentration of deliveries were 20×10^6 apoptotic cells ±2 µg LPS (Sigma-Aldrich), ±10 µg Poly I:C (InvivoGen), 1 µg sOVA (Sigma-Aldrich), and 30×10^6 of 0.5-, 1-, 2-, 3-, and 4.5-µm yellow-green carboxylated beads (Polysciences). In co-delivery experiments, 20×10^6 apoptotic cells and 30×10^6 2-µm beads were administered i.n. Mice were sacrificed at various times dependent on experimental design.

Apoptotic cell delivery. Thymocytes were obtained from C57BL/6 and BALB/c mice 7–8 wk of age. Single-cell suspensions were made using the rubber end of a syringe and mashing cells through a 40-µm nylon filter. Apoptosis of murine thymocytes and murine lung epithelial cells (MLE 12; American Type Culture Collection) was induced by 60 mJ UV radiation exposure (StrataLinker 1800; Agilent Technologies) followed by 2-h (for thymocytes) and 3-h (for epithelial cells) incubation at 37°C in RPMI + 10% FCS. Apoptosis of human neutrophils was induced by aging the cells overnight at 5×10^6 cells/ml in RPMI + 10% FBS at 37°C in 5% CO_2 in a 25-cm^2 TC flask (Frasch et al., 2011). Phosphatidylserine exposure was detected by Annexin V staining and propidium iodide (PI) to assure that no necrotic cells were present before delivery. 2 h (for thymocytes) or 3 h (for epithelial cells) after UV exposure, cells were 60% apoptotic Annexin V^+ PI^-, 40% were Annexin V^- PI^- (but with time these cells would all become apoptotic), and <0.2% were PI^+. Apoptotic cells were labeled with 10 µM CFSE (Invitrogen) and then resuspended and washed three times in 30 ml RPMI + 10% FCS before delivery.

Proliferation of OVA-specific transgenic $CD8^+$ and $CD4^+$ T cells. Spleen cells from OT-1 and OT-2 mice, in which the TCR of $CD8^+$ and $CD4^+$ cells are restricted to OVA were isolated and labeled with 10 µM CFSE. Half a million of these cells were transferred i.v. into recipient mice 1 d before i.n. delivery of apoptotic cells and sOVA. Mice were sacrificed 3 d after i.n. deliveries for analysis of T cell proliferation (CFSE dye dilution) in the LLN and intracellular cytokine staining.

Intracellular cytokine staining. LLNs isolated 3 d after i.n. deliveries of apoptotic cells or sOVA ± Poly I:C were teased and digested in Collagenase D for 30 min and then pressed through a 100-µm nylon filter to obtain single-cell suspensions of APCs and proliferating T cells. Isolated cells were cultured for 5 h in RPMI + 10% FCS containing 10 µM $OVA_{257–264}$ and 10 µM $OVA_{323–339}$ and 10 µg/ml Brefeldin A. After surface staining, cells were fixed in 4% paraformaldehyde and then blocked and permeabilized with PBS-saponin/milk. Cells were stained with APC conjugated to IFN-γ or isotype control (BD).

In vivo cytotoxic T cell assay. 1 d after OT-1 cell adoptive transfer, WT mice were administered by i.n. delivery with WT apoptotic or OVA apoptotic cells ± 10 µg Poly I:C. 6 d after immunization, labeled WT and OVA splenocytes were injected i.v. WT spleen cells were labeled with 1 µM CFSE, and spleen cells from actin-OVA^+ mice were labeled with 10 µM CFSE. Labeled splenocytes were mixed in a 1:1 ratio before i.v. delivery of 10^7 cells/mouse. The next day, spleens were harvested to acquire single-cell suspensions, and specific killing of adoptively transferred $CFSE^+$ low and high populations was assessed by flow cytometry.

Microscopy. Pulmonary DC subsets were FACS sorted (MoFlo; Beckman Coulter) from whole lung digests 2 h after CFSE-labeled apoptotic thymocytes were delivered i.n. Sorted DCs were stained with Image-iT LIVE plasma membrane and nuclear labeling kit (Invitrogen), and then cytospins were performed to deposit cells on positively charged glass slides. Images were obtained using an AxioVision microscope (Carl Zeiss), and efferocytic DCs were quantified using AxioVision digital imaging software (Carl Zeiss). DCs were considered efferocytic if $CFSE^+$ vesicles were detected within the cellular membrane. To determine the percentage of $CFSE^+$ DCs, 30–60 cells were counted in 25 randomized fields of view per sample.

Isolation of splenic and lung DCs for in vitro analysis. From single-cell suspensions, isolation of CD45.2 splenic and lung DCs was performed using CD11c microbeads from Miltenyi Biotec. Miltenyi Biotec instruction for CD11c cell isolation was carefully followed. Triplicates of 1×10^5 DCs were cultured in 96-well flat-bottom plates in RPMI + 5% FCS, 50 µM mercaptoethanol, L-glutamine, streptomycin, and penicillin and allowed to rest for 1 h. After 1 h, Pacific blue succinimidyl ester (PBSE; Invitrogen)–labeled CD45.1 apoptotic thymocytes were cultured for 4 h at 37°C. After incubation, cells were harvested and stained for DC subsets from the lung and spleen. A final concentration of 1 mM EDTA was added to promote nonadherence of apoptotic cells on DCs. In addition, analysis to exclude externally adhered apoptotic cells on DCs was performed by excluding DCs expressing CD45.1.

In vivo analysis of splenic DC migration CD45.2 splenic DC subsets were sorted using the BD Aria. Intradermal injections of splenic DCs were placed into the back skin of CD45.1 mice. 24 h after injection, skin-draining LNs were harvested, digested, and analyzed for DC migration. From single-cell suspensions of CD45.2 $CX3CR1^{gfp/gfg}$ mice, isolation of the CD45.2 splenic DCs was performed using CD11b microbeads from Miltenyi Biotec, followed by sorting GFP^{hi} and GFP^{lo} DC–expressing subsets using the BD Aria.

Gene array. Whole-mouse genome Affymetrix gene arrays were performed with the Immunological Genome Project (ImmGen) at Harvard University (Heng and Painter, 2008). As per the specifications of ImmGen, we followed a standard operation procedure for the isolation and purification of all cell populations that is uniform across the ImmGen dataset. Procedures for cell isolation, sorting, and RNA extractions are outlined in extensive detail at http://www.immgen.org. Briefly, PBS-perfused lungs and spleens were digested using 1.75 mg/ml Liberase Blendzyme 3 (Roche) for 15 min, filtered twice through a 100-µm nylon strainer, washed with HBSS, and then stained with conjugated flow cytometry antibodies (eBioscience) to identify pulmonary DCs, pulmonary macrophages, splenic DCs, and splenic T cells. PI was used to exclude dead cells. Cell populations were sorted twice to enhance purity (BD Aria). The entire procedure from the time of sacrifice to cells collected in TRIZOL was completed in <3 h, which is a requirement by ImmGen. Flow plots of the actual sorts and cells used for RNA extraction

may be viewed at http://www.immen.org. All datasets have been deposited in GEO DataSets under accession no. GSE15907. Validation for the use of pulmonary DC gene arrays was assessed by the confirmation of mRNA expression for known surface proteins, transcription factors, and growth factors associated with pulmonary DCs and controls to compare with splenic DCs, pulmonary macrophages, and splenic CD4 T cells (Table S2).

Statistics. Statistical analysis was conducted using InStat and Prism software (both from GraphPad Software). All results are expressed as the mean ± SEM. Statistical tests were performed using two-tailed Student's *t* test. A value of $P < 0.05$ was considered statistically significant.

Online supplemental material. Fig. S1 displays the gating strategy for $CFSE^+$ DCs in the LLN 24 h after i.n. delivery of CFSE-labeled apoptotic BALB/c thymocytes, human neutrophils, or murine lung epithelial cells (MLE 12). Fig. S2 demonstrates that splenic $CD8^+$ DCs do not migrate down afferent lymphatics. Table S1, included as a separate PDF file, shows gene expression analysis for candidate phosphatidylserine receptors, bridging molecules, Toll-like receptors, and chemokine receptors for pulmonary DCs, pulmonary macrophages, and splenic CD4 T cells. Table S2, included as a separate PDF file, validates gene array for known protein expression associated with pulmonary DCs, splenic DCs, pulmonary macrophages, and splenic CD4 T cells. Online supplemental material is available at http://www.jem.org/cgi/content/full/jem.20110538/DC1.

Thank you to the ImmGen Project team, which is supported by National Institutes of Health (NIH) grant R24 AI072073 to the Immunological Genome Project.

Grant support from the NIH was given to C.V. Jakubzick and P.M. Henson (NHLBI-HL81151 and NIGMS-GM61031) and G.J. Randolph (NIAID-AI049653). K. Shortman, M.H. Lahoud, and I. Caminschi are supported by the National Health and Medical Research Council of Australia.

The authors have no conflicting financial interests.

Submitted: 17 March 2011
Accepted: 26 July 2011

REFERENCES

Ballesteros-Tato, A., B. León, F.E. Lund, and T.D. Randall. 2010. Temporal changes in dendritic cell subsets, cross-priming and costimulation via CD70 control CD8(+) T cell responses to influenza. *Nat. Immunol.* 11:216–224. doi:10.1038/ni.1838

Bedoui, S., P.G. Whitney, J. Waithman, L. Eidsmo, L. Wakim, I. Caminschi, R.S. Allan, M. Wojtasiak, K. Shortman, F.R. Carbone, et al. 2009. Cross-presentation of viral and self antigens by skin-derived CD103+ dendritic cells. *Nat. Immunol.* 10:488–495. doi:10.1038/ni.1724

Belz, G.T., C.M. Smith, L. Kleinert, P. Reading, A. Brooks, K. Shortman, F.R. Carbone, and W.R. Heath. 2004. Distinct migrating and nonmigrating dendritic cell populations are involved in MHC class I-restricted antigen presentation after lung infection with virus. *Proc. Natl. Acad. Sci. USA.* 101:8670–8675. doi:10.1073/pnas.0402644101

Belz, G.T., S. Bedoui, F. Kupresanin, F.R. Carbone, and W.R. Heath. 2007. Minimal activation of memory CD8+ T cell by tissue-derived dendritic cells favors the stimulation of naive CD8+ T cells. *Nat. Immunol.* 8:1060–1066. doi:10.1038/ni1505

Caminschi, I., A.I. Proietto, F. Ahmet, S. Kitsoulis, J. Shin Teh, J.C. Lo, A. Rizzitelli, L. Wu, D. Vremec, S.L. van Dommelen, et al. 2008. The dendritic cell subtype-restricted C-type lectin Clec9A is a target for vaccine enhancement. *Blood.* 112:3264–3273. doi:10.1182/blood-2008-05-155176

deCathelineau, A.M., and P.M. Henson. 2003. The final step in programmed cell death: phagocytes carry apoptotic cells to the grave. *Essays Biochem.* 39:105–117.

del Rio, M.L., J.I. Rodriguez-Barbosa, E. Kremmer, and R. Förster. 2007. CD103- and CD103+ bronchial lymph node dendritic cells are specialized in presenting and cross-presenting innocuous antigen to CD4+ and CD8+ T cells. *J. Immunol.* 178:6861–6866.

Dudziak, D., A.O. Kamphorst, G.F. Heidkamp, V.R. Buchholz, C. Trumpfheller, S. Yamazaki, C. Cheong, K. Liu, H.W. Lee, C.G. Park, et al. 2007. Differential antigen processing by dendritic cell subsets in vivo. *Science.* 315:107–111. doi:10.1126/science.1136080

Edelson, B.T., W. Kc, R. Juang, M. Kohyama, L.A. Benoit, P.A. Klekotka, C. Moon, J.C. Albring, W. Ise, D.G. Michael, et al. 2010. Peripheral $CD103^+$ dendritic cells form a unified subset developmentally related to $CD8\alpha^+$ conventional dendritic cells. *J. Exp. Med.* 207:823–836. doi:10.1084/jem.20091627

Frasch, S.C., R.F. Fernandez-Boyanapalli, K.Z. Berry, C.C. Leslie, J.V. Bonventre, R.C. Murphy, P.M. Henson, and D.L. Bratton. 2011. Signaling via macrophage G2A enhances efferocytosis of dying neutrophils by augmentation of Rac activity. *J. Biol. Chem.* 286:12108–12122. doi:10.1074/jbc.M110.181800

GeurtsvanKessel, C.H., M.A. Willart, L.S. van Rijt, F. Muskens, M. Kool, C. Baas, K. Thielemans, C. Bennett, B.E. Clausen, H.C. Hoogsteden, et al. 2008. Clearance of influenza virus from the lung depends on migratory $langerin^+CD11b^-$ but not plasmacytoid dendritic cells. *J. Exp. Med.* 205:1621–1634. doi:10.1084/jem.20071365

GeurtsvanKessel, C.H., M.A. Willart, I.M. Bergen, L.S. van Rijt, F. Muskens, D. Elewaut, A.D. Osterhaus, R. Hendriks, G.F. Rimmelzwaan, and B.N. Lambrecht. 2009. Dendritic cells are crucial for maintenance of tertiary lymphoid structures in the lung of influenza virus–infected mice. *J. Exp. Med.* 206:2339–2349. doi:10.1084/jem.20090410

Ginhoux, F., K. Liu, J. Helft, M. Bogunovic, M. Greter, D. Hashimoto, J. Price, N. Yin, J. Bromberg, S.A. Lira, et al. 2009. The origin and development of nonlymphoid tissue $CD103^+$ DCs. *J. Exp. Med.* 206:3115–3130. doi:10.1084/jem.20091756

Heng, T.S., and M.W. Painter; Immunological Genome Project Consortium. 2008. The Immunological Genome Project: networks of gene expression in immune cells. *Nat. Immunol.* 9:1091–1094. doi:10.1038/ni1008-1091

Hildner, K., B.T. Edelson, W.E. Purtha, M. Diamond, H. Matsushita, M. Kohyama, B. Calderon, B.U. Schraml, E.R. Unanue, M.S. Diamond, et al. 2008. Batf3 deficiency reveals a critical role for CD8alpha+ dendritic cells in cytotoxic T cell immunity. *Science.* 322:1097–1100. doi:10.1126/science.1164206

Iyoda, T., S. Shimoyama, K. Liu, Y. Omatsu, Y. Akiyama, Y. Maeda, K. Takahara, R.M. Steinman, and K. Inaba. 2002. The $CD8^+$ dendritic cell subset selectively endocytoses dying cells in culture and in vivo. *J. Exp. Med.* 195:1289–1302. doi:10.1084/jem.20020161

Jakubzick, C., and G.J. Randolph. 2010. Methods to study pulmonary dendritic cell migration. *Methods Mol. Biol.* 595:371–382. doi:10.1007/978-1-60761-421-0_24

Jakubzick, C., J. Helft, T.J. Kaplan, and G.J. Randolph. 2008a. Optimization of methods to study pulmonary dendritic cell migration reveals distinct capacities of DC subsets to acquire soluble versus particulate antigen. *J. Immunol. Methods.* 337:121–131. doi:10.1016/j.jim.2008.07.005

Jakubzick, C., F. Tacke, F. Ginhoux, A.J. Wagers, N. van Rooijen, M. Mack, M. Merad, and G.J. Randolph. 2008b. Blood monocyte subsets differentially give rise to CD103+ and CD103− pulmonary dendritic cell populations. *J. Immunol.* 180:3019–3027.

Kim, T.S., and T.J. Braciale. 2009. Respiratory dendritic cell subsets differ in their capacity to support the induction of virus-specific cytotoxic CD8+ T cell responses. *PLoS ONE.* 4:e4204. doi:10.1371/journal.pone.0004204

Kirby, A.C., J.G. Raynes, and P.M. Kaye. 2006. CD11b regulates recruitment of alveolar macrophages but not pulmonary dendritic cells after pneumococcal challenge. *J. Infect. Dis.* 193:205–213. doi:10.1086/498874

Landsman, L., C. Varol, and S. Jung. 2007. Distinct differentiation potential of blood monocyte subsets in the lung. *J. Immunol.* 178:2000–2007.

Lukens, M.V., D. Kruijsen, F.E. Coenjaerts, J.L. Kimpen, and G.M. van Bleek. 2009. Respiratory syncytial virus-induced activation and migration of respiratory dendritic cells and subsequent antigen presentation in the lung-draining lymph node. *J. Virol.* 83:7235–7243. doi:10.1128/JVI.00452-09

Maldonado-López, R., T. De Smedt, P. Michel, J. Godfroid, B. Pajak, C. Heirman, K. Thielemans, O. Leo, J. Urbain, and M. Moser. 1999. $CD8\alpha^+$ and $CD8\alpha^-$ subclasses of dendritic cells direct the development of distinct T helper cells in vivo. *J. Exp. Med.* 189:587–592. doi:10.1084/jem.189.3.587

Plantinga, M., H. Hammad, and B.N. Lambrecht. 2010. Origin and functional specializations of DC subsets in the lung. *Eur. J. Immunol.* 40:2112–2118. doi:10.1002/eji.201040562

Qiu, C.H., Y. Miyake, H. Kaise, H. Kitamura, O. Ohara, and M. Tanaka. 2009. Novel subset of CD8alpha+ dendritic cells localized in the marginal zone is responsible for tolerance to cell-associated antigens. *J. Immunol.* 182:4127–4136. doi:10.4049/jimmunol.0803364

Smith, A.L., and B. Fazekas de St Groth. 1999. Antigen-pulsed CD8α^+ dendritic cells generate an immune response after subcutaneous injection without homing to the draining lymph node. *J. Exp. Med.* 189:593–598. doi:10.1084/jem.189.3.593

Sung, S.S., S.M. Fu, C.E. Rose Jr., F. Gaskin, S.T. Ju, and S.R. Beaty. 2006. A major lung CD103 (alphaE)-beta7 integrin-positive epithelial dendritic cell population expressing Langerin and tight junction proteins. *J. Immunol.* 176:2161–2172.

Vermaelen, K., and R. Pauwels. 2004. Accurate and simple discrimination of mouse pulmonary dendritic cell and macrophage populations by flow cytometry: methodology and new insights. *Cytometry A.* 61A:170–177. doi:10.1002/cyto.a.20064

Wakim, L.M., and M.J. Bevan. 2011. Cross-dressed dendritic cells drive memory CD8+ T-cell activation after viral infection. *Nature.* 471:629–632. doi:10.1038/nature09863